Journal of Catalysis **186,** 310–317 (1999)
Article ID jcat.1999.2559, available online at http://www.idealibrary.com on IDEAL®

Partial Oxidation of Toluene over Ultrafine Mixed Mo-Based Oxide Particles

Wenxing Kuang, Yining Fan, Kaidong Chen, and Yi Chen

Department of Chemistry, Nanjing University, Nanjing 210093, China

Received January 5, 1999; revised May 7, 1999; accepted May 13, 1999

The structure and catalytic properties of ultrafine Mo-based oxide particles prepared by the sol–gel technique are studied by using XRD, TEM, TPR, FT-Raman, BET surface area measurement, and microreactor tests. It is shown that for partial oxidation of toluene to benzaldehyde, the ultrafine $Fe_2(MoO_4)_3$ and $Ce_2(MoO_4)_3$ particles exhibit higher benzaldehyde selectivity and toluene conversion than the corresponding larger oxide particles prepared by the conventional coprecipitation method. The unique catalytic properties of ultrafine $Fe_2(MoO_4)_3$ and $Ce_2(MoO_4)_3$ particles may be correlated to the higher mobility of lattice oxygen ions in the oxides and their higher BET surface area. For the ultrafine Mo-based oxides prepared by the sol–gel process, the selectivity to benzaldehyde follows the order $Ce_2(MoO_4)_3 > Fe_2(MoO_4)_3 > La_2(MoO_4)_3 > MoO_3$, which is in good agreement with the reducibility of Mo ions and reactivity of lattice oxygen ions in the ultrafine Mo-based oxides. These results reveal that the lattice oxygen ions in the Mo-based oxides are the main active species for partial oxidation of toluene to benzaldehyde. The results of *in situ* LRS studies indicate that the terminal Mo=O bonds in $Ce_2(MoO_4)_3$ are the main reactive species for partial oxidation of toluene to benzaldehyde.

Key Words: **ultrafine particles; Mo-based oxides; partial oxidation of toluene.**

INTRODUCTION

Partial oxidation of hydrocarbons via gas-phase process is one of the most attractive and difficult challenges in the fields of heterogeneous catalysis. About a quarter of the industrial production of monomers and chemical intermediates is made by the partial oxidation process. Partial oxidation of toluene to benzaldehyde is among the most extensively investigated systems because it was chosen as a model reaction for the study of oxidation kinetics and methods to predict optimum reactor design and operation conditions in which a complex reaction system is involved (1). The significance of this process for the chemical industry has been long perceived and many efforts have been made in improving catalytic selectivity in the past decades (2–22). However, the direct utilization of this reaction for the manufacture of benzaldehyde has remained extremely difficult.

As might be expected, mixed metal oxides have been among the most widely studied catalysts used for partial oxidation of toluene. It has been found that of these oxide catalysts, higher activity and improved selectivity for the partial oxidation of toluene are generally achieved by the Mo-based and V-based oxides (2–19), and the preparation conditions, oxide composition, and catalyst structure exert great influences on the catalytic selectivity. The most common methods employed for the synthesis of the oxide catalysts are the coprecipitation and solid-state reaction routes (23), which transform into mixed oxide at high temperature. However, the size of the oxide particles prepared by these conventional methods is very large, and the BET surface area is rather small. This obviously limits the catalytic activity of these oxide catalysts.

In the past decade, ultrafine particles have attracted considerable attention in terms of heterogeneous catalysis owing to their unique physical and chemical properties (24–27). They are expected to have unique catalytic properties because of their nano-scale particle size. Among various methods for the preparation of ultrafine oxide particles, the sol–gel technique has received increasing attention lately due to its potential in delivering samples that are better mixed on a molecular scale, which provides an opportunity for tailoring the chemical and structural properties of oxide catalysts (28–31). For instance, the metal oxides prepared by the sol–gel process have several properties that make them promising catalyst materials, such as stabilized surface area, strong thermal stability, large ion exchange capacity, and dual ion exchange properties for cations and anions (32, 33).

In our previous studies (34, 35), ultrafine mixed Mo-based oxide particles were prepared by the sol–gel method, and it was found that by decreasing the particle size of the Mo-based oxide to nano-scale, the catalytic activity for partial oxidation of toluene to benzaldehyde could be remarkably improved. In the present work, we further study the structure and catalytic properties of the ultrafine Mo-based oxides prepared by the sol–gel technique. The state and reactivity of lattice oxygen ions in the ultrafine Mo-based oxides have been explored.

EXPERIMENTAL

Sample Preparation

Ultrafine mixed Mo-based oxide particles were prepared by the sol–gel method as reported in our previous studies

0021-9517/99 $30.00

(34), in which citric acid was used as a complexing polyfunctional hydroxyacid. Nitrate iron (nitrate cerium, nitrate lanthanum), ammonium molybdate, and citric acid (the molar ratio of citric acid to metallic ions is 1 : 3) were dissolved in deionized water separately and mixed together. The pH of the mixture solutions was adjusted to lower than 1.0 for the Fe–Mo and Ce–Mo samples, and to ca. 1.5 for the La–Mo sample. The above solutions were kept in a water bath at 333 K for gelation. The gels thus prepared were first dried at 393 K and then calcined to afford the oxide catalysts. The mono-component Fe_2O_3, CeO_2, La_2O_3, and MoO_3 oxides were prepared by the same procedures. For comparison, the conventional coprecipitation method was also used to prepare Fe–Mo and Ce–Mo samples as described in the literature (23).

Characterization

X-ray diffraction patterns were obtained in a Shimadzu-3A diffractometer with Fe $K\alpha$ radiation (0.19373 nm) for Fe_2O_3 and $Fe_2(MoO_4)_3$ samples, and Cu $K\alpha$ radiation (0.15418 nm) for other samples. The particles' shapes and sizes were elucidated by TEM with a JEM-100S transmission electron microscope. The distribution of the oxide particle sizes was determined by the TEM images. The BET surface area measurements were performed on a micromeritics ASAP-2000 instrument (N_2 adsorption at 77 K). The TPR experiments were carried out in a U-type quartz reactor with a heating rate of 10 K min^{-1} and a flow rate of H_2–Ar mixture (5.0 vol% hydrogen) of ca. 30 ml min^{-1}. Hydrogen consumption was monitored by a thermal conductivity detector. The pulse microreactor combined with *in situ* Raman spectroscopy experiments were performed using a specially designed *in situ* cell. The oxide was placed in the cell, which was aligned using the cell holder in the sample compartment of the spectrometer. FT-Raman spectra were taken with a Bruker RSF 100 spectrometer fitted with an InGaAs detector cooled by liquid nitrogen. Raman excitation at 1064 nm was provided by an Na : YAG laser.

Catalytic Oxidation of Toluene

The toluene oxidation reaction was used as a probe to study the catalytic properties of the ultrafine Mo-based oxides. The oxides (250 mg) were introduced into a U-type quartz fixed bed microreactor, and their catalytic properties for partial oxidation of toluene to benzaldehyde were evaluated under the reaction conditions of 0.1 MPa, 673 K, helium/oxygen/toluene = 50/5/1 (vol/vol/vol), helium flowrate 20 ml min^{-1}, $W/F = 570$ (g catalyst/toluene mole flow in mole/h). The reaction products were analyzed by on-line gas chromatography. Under the above reaction conditions, the main products were mainly CO, CO_2, H_2O, and benzaldehyde.

The reactivity of lattice oxygen ions in the ultrafine Mo-based oxides in the absence of molecular oxygen was determined in a pulse microreactor under the conditions 623 K, 0.2 MPa, helium flow rate of 40 ml min^{-1}, and 0.81 μmol toluene every pulse (35–36).

RESULTS AND DISCUSSION

The Structure of the Ultrafine Mo-Based Oxides

XRD, TEM, and BET surface area measurements were used for the Mo-based oxide characterization. The structure, particle size, and BET surface area of various samples are presented in Table 1. It was found that forming crystalline Fe_2O_3, CeO_2, La_2O_3, MoO_3, $Fe_2(MoO_4)_3$, $Ce_2(MoO_4)_3$, and $La_2(MoO_4)_3$ by the sol–gel technique needed calcination at 673, 673, 773, 673, 673, 673, and 773 K, respectively; forming crystalline $Fe_2(MoO_4)_3$ and $Ce_2(MoO_4)_3$ from their precipitates needed calcination at 773 and 823 K, respectively (34, 37). It can be seen that the size of Fe_2O_3, CeO_2, and La_2O_3 particles is in the range ca. 40–80, 10–20, and 40–80 nm, respectively, while the size of MoO_3 particles is larger than 100 nm. This reveals that ultrafine Fe_2O_3, CeO_2, and La_2O_3 particles can be obtained by the sol–gel method.

With addition of iron, cerium, and lanthanum oxides to molybdenum oxide, however, the size of $Fe_2(MoO_4)_3$, $Ce_2(MoO_4)_3$, and $La_2(MoO_4)_3$ particles is in the range ca. 20–60, 20–40, and 40–80 nm, respectively. The BET surface areas of $Fe_2(MoO_4)_3$, $Ce_2(MoO_4)_3$, and $La_2(MoO_4)_3$ are 20.2, 20.3, and 15.4 $m^2 g^{-1}$, respectively. Due to the molecular homogeneous distribution of various components in the sol–gel process (28–31), it is possible to form ultrafine mixed Mo-based oxide particles from the gels. $Fe_2(MoO_4)_3$, $Ce_2(MoO_4)_3$, and $La_2(MoO_4)_3$ prepared by the sol–gel method are actually ultrafine oxide particles (<100 nm). In contrast, it can be found that the size of $Fe_2(MoO_4)_3$ and $Ce_2(MoO_4)_3$ particles prepared by the coprecipitation method is much larger than the size of those prepared by the sol–gel technique.

TABLE 1

The Structure, Particle Size, and BET Surface Area of Various Samples

Sample	Preparation method	Calcination temperature (K)	Particle size (nm)	BET surface area ($m^2 g^{-1}$)
Fe_2O_3	sol–gel	673	40–80	10.3
CeO_2	sol–gel	673	10–20	41.0
La_2O_3	sol–gel	773	40–80	15.0
MoO_3	sol–gel	673	>100	5.1
$Fe_2(MoO_4)_3$	sol–gel	673	20–60	20.2
$Ce_2(MoO_4)_3$	sol–gel	673	20–40	20.3
$La_2(MoO_4)_3$	sol–gel	773	40–80	15.4
$Fe_2(MoO_4)_3$	coprecipitation	773	>200	2.7
$Ce_2(MoO_4)_3$	coprecipitation	823	>100	4.2

TABLE 2

The Catalytic Properties of Various Samples for Partial Oxidation of Toluene

Sample	Conversion of toluene (mol%)	Benzaldehyde selectivity (%)	Benzaldehyde yield (mol%)	Specific activity (μmol s^{-1} m^{-2})
Fe_2O_3[a]	73.3	0	0	0
CeO_2[a]	63.4	0	0	0
La_2O_3[b]	64.0	0	0	0
MoO_3[a]	36.3	17.9	6.5	0.0061
$Fe_2(MoO_4)_3$[a]	65.8	39.8	26.2	0.0063
$Ce_2(MoO_4)_3$[a]	60.3	52.3	31.5	0.0075
$La_2(MoO_4)_3$[b]	55.8	30.8	17.2	0.0054
$Fe_2(MoO_4)_3$[c]	49.0	21.7	10.6	0.0191
$Ce_2(MoO_4)_3$[d]	58.2	19.1	11.1	0.0128

[a] Prepared by the sol–gel method and calcined at 673 K.
[b] Prepared by the sol–gel method and calcined at 773 K.
[c] Prepared by the coprecipitation method and calcined at 773 K.
[d] Prepared by the coprecipitation method and calcined at 823 K.

Catalytic Properties for Partial Oxidation of Toluene

The catalytic properties of ultrafine mixed Mo-based oxide particles for partial oxidation of toluene to benzaldehyde are listed in Table 2. For Fe_2O_3, CeO_2, and La_2O_3 samples, no partial oxidation product is detected under our reaction conditions, suggesting that these oxides are catalysts for complete oxidation of toluene. These results are consistent with those reported in the literature (38, 39). This is not the case for the MoO_3 sample, which exhibits selectivity for benzaldehyde, suggesting that molybdenum oxide is the catalytic active species for partial oxidation of toluene.

By adding iron, cerium, and lanthanum oxides to MoO_3, however, both the conversion of toluene and the selectivity to benzaldehyde are improved remarkably, so that the ultrafine Mo-based oxides show higher benzaldehyde yield than the mono-component MoO_3 catalyst. The addition of different promoter oxides results in different catalytic properties of the ultrafine Mo-based oxides. The catalytic activity for toluene oxidation (conversion of toluene per BET surface area) follows the order $Fe_2O_3 \sim MoO_3 > La_2O_3 > La_2(MoO_4)_3 > Fe_2(MoO_4)_3 > Ce_2(MoO_4)_3 > CeO_2$. It is well known that for partial oxidation of hydrocarbons, the higher the BET surface area of the oxide catalysts, the higher the conversion of hydrocarbons. Thus it may be concluded that the higher toluene conversion of the ultrafine Mo-based oxide particles may be mainly correlated to their higher BET surface area. The selectivity to benzaldehyde follows the order $Ce_2(MoO_4)_3 > Fe_2(MoO_4)_3 > La_2(MoO_4)_3 > MoO_3$; the specific activity follows the order $Ce_2(MoO_4)_3 > Fe_2(MoO_4)_3 \sim MoO_3 > La_2(MoO_4)_3$. This indicates that cerium oxide is the most effective promoter oxide for improving catalytic activity for partial oxidation of toluene to benzaldehyde.

For comparison, the catalytic properties of the large $Fe_2(MoO_4)_3$ and $Ce_2(MoO_4)_3$ particles prepared by the coprecipitation method are also listed in Table 2. It is found that both the benzaldehyde selectivity and the benzaldehyde yield of ultrafine oxide particles are much higher than those of large oxide particles. These results reveal that ultrafine Mo-based oxide particles have unique catalytic activity for partial oxidation of toluene. However, the specific activity of the ultrafine Mo-based oxide particles is lower than that of the corresponding large oxide particles. This reveals that the higher toluene conversion and benzaldehyde yield of the ultrafine Mo-based oxide particles may be correlated to their higher BET surface area. The influence of calcination temperature on the catalytic properties of the Mo-based oxide catalysts for partial oxidation of toluene to benzaldehyde is shown in Table 3. It can be found that for $Fe_2(MoO_4)_3$ and $Ce_2(MoO_4)_3$ prepared by the sol–gel and coprecipitation methods, both the benzaldehyde yield and specific activity decrease rapidly with the increase of the calcination temperatures.

Reduction Behavior of the Ultrafine Mo-Based Oxides

The TPR profiles of the mono-component oxides and the ultrafine Mo-based oxides are shown in Figs. 1 and 2, respectively. For Fe_2O_3, two hydrogen consumption peaks at ca. 660 and 857 K are seen, and can be assigned to the reduction of Fe_2O_3 to Fe_3O_4 and of Fe_3O_4 to α-Fe, respectively (40). For CeO_2, two very weak hydrogen consumption peaks at ca. 783 and 1049 K are observed; for La_2O_3, a very weak hydrogen consumption peak at ca. 943 K is observed. This indicates that the reduction of CeO_2 and

TABLE 3

The Catalytic Properties of Various Samples Calcined at Different Temperatures for Partial Oxidation of Toluene

Sample	Conversion of toluene (mol%)	Benzaldehyde selectivity (%)	Benzaldehyde yield (mol%)	Specific activity (μmol s^{-1} m^{-2})
$Fe_2(MoO_4)_3$[a]	65.8	39.8	26.2	0.0063
$Fe_2(MoO_4)_3$[b]	58.2	30.1	17.5	0.0045
$Fe_2(MoO_4)_3$[c]	40.9	10.2	4.17	0.0038
$Ce_2(MoO_4)_3$[a]	60.3	52.3	31.5	0.0075
$Ce_2(MoO_4)_3$[b]	45.6	38.4	17.5	0.0064
$Ce_2(MoO_4)_3$[c]	45.7	28.5	13.0	0.0053
$Fe_2(MoO_4)_3$[d]	49.0	21.7	10.6	0.0191
$Fe_2(MoO_4)_3$[e]	51.6	14.5	7.48	0.0145
$Ce_2(MoO_4)_3$[e]	58.2	19.1	11.1	0.0128
$Ce_2(MoO_4)_3$[f]	54.8	13.9	7.6	0.0095

[a] Prepared by the sol–gel method and calcined at 673 K.
[b] Prepared by the sol–gel method and calcined at 773 K.
[c] Prepared by the sol–gel method and calcined at 873 K.
[d] Prepared by the coprecipitation method and calcined at 773 K.
[e] Prepared by the coprecipitation method and calcined at 823 K.
[f] Prepared by the coprecipitation method and calcined at 873 K.

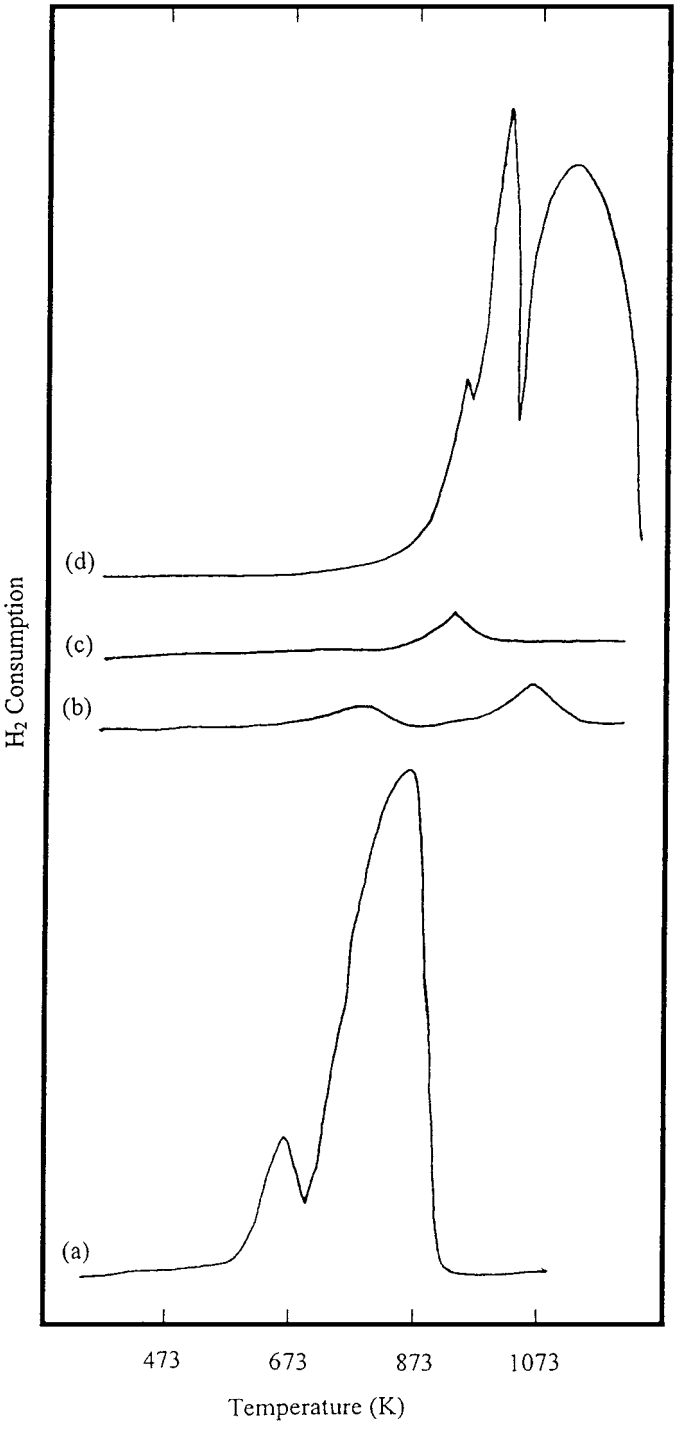

FIG. 1. TPR profiles of the mono-component oxide catalysts: (a) Fe_2O_3, (b) CeO_2, (c) La_2O_3, (d) MoO_3.

La_2O_3 particles is very difficult. As reported by Guerrero-Ruiz *et al.* (41), the hydrogen consumption at lower temperature can be due to the reduction of surface ions, while the reduction peak at higher temperature can be due to the elimination of bulk oxygen anions. For MoO_3, three hydrogen consumption peaks at ca. 953, 1026, and 1143 K are observed, and can be distributed to the reduction of MoO_3 to $MoO_{2.8}$, of $MoO_{2.8}$ to Mo_4O_{11}, and of Mo_4O_{11} to MoO_2, respectively (42).

As shown in Fig. 2, compared with that of mono-component oxides, due to the formation of crystalline $Fe_2(MoO_4)_3$, $Ce_2(MoO_4)_3$, and $La_2(MoO_4)_3$, the reduction

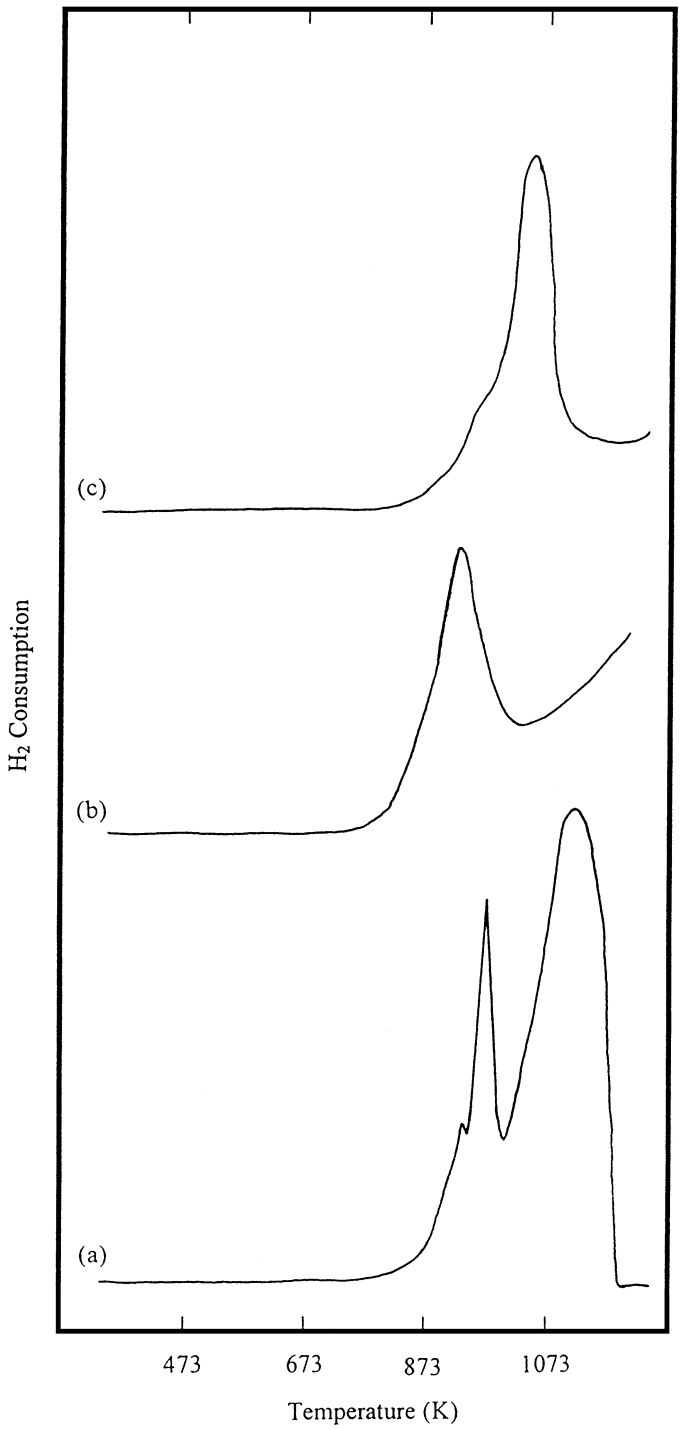

FIG. 2. TPR profiles of the ultrafine mixed Mo-based oxides: (a) $Fe_2(MoO_4)_3$, (b) $Ce_2(MoO_4)_3$, (c) $La_2(MoO_4)_3$.

behavior of the ultrafine Mo-based oxides is quite different. For $Fe_2(MoO_4)_3$, three hydrogen consumption peaks at ca. 928, 975, and 1139 K are observed, and might be mainly distributed to the reduction of $Fe_2(MoO_4)_3$ to β-$FeMoO_4$ and Mo_4O_{11}, of β-$FeMoO_4$ and Mo_4O_{11} to $Fe_2Mo_3O_8$ and MoO_2, and of $Fe_2Mo_3O_8$ and MoO_2 to Fe^0, Mo^0, and Fe_3Mo, respectively (43, 44). For $Ce_2(MoO_4)_3$, a hydrogen consumption peak at ca. 927 K is seen and can be assigned to the reduction of $Ce_2(MoO_4)_3$ to $Ce_2Mo_3O_9$ (45). For $La_2(MoO_4)_3$, two hydrogen consumption peaks at ca. 963 and 1058 K are observed and can be assigned to the reduction of the surface and bulk of $La_2(MoO_4)_3$ to $La_2Mo_3O_9$, respectively (45).

Comparing the reduction behavior of MoO_3 and the ultrafine Mo-based oxides, it can be found that for the reduction of Mo^{6+} to Mo^{4+} in the oxides, the peak maximums of MoO_3, $Fe_2(MoO_4)_3$, $Ce_2(MoO_4)_3$, and $La_2(MoO_4)_3$ are at 1143, 975, 927, and 1058 K, respectively. Compared with that of MoO_3, the peak maximums of $La_2(MoO_4)_3$, $Fe_2(MoO_4)_3$, and $Ce_2(MoO_4)_3$ shift in order to lower temperatures, respectively. This suggests that due to the formation of bicomponent oxides of $Fe_2(MoO_4)_3$, $Ce_2(MoO_4)_3$, and $La_2(MoO_4)_3$, the reduction of Mo ions in the ultrafine oxides is easier. For the reduction of Mo^{6+} to Mo^{4+} in the oxides, the reducibility of the above four samples follows the order $Ce_2(MoO_4)_3 > Fe_2(MoO_4)_3 > La_2(MoO_4)_3 > MoO_3$, which is in good agreement with their selectivity to benzaldehyde. This implies that the selectivity to benzaldehyde of the ultrafine Mo-based oxides is closely correlated to the reducibility of Mo ions in the ultrafine Mo-based oxides. The easier the reduction of Mo ions in the oxides, the higher the selectivity to benzaldehyde.

As reported in our previous study (37), compared with that for ultrafine $Fe_2(MoO_4)_3$ particles, the corresponding hydrogen consumption peaks (shown in Fig. 3) for large $Fe_2(MoO_4)_3$ particles prepared by the coprecipitation method shift to higher temperatures, 958, 1018, and 1191 K, respectively. This result indicates that with the decrease of the oxide particle size to nano-scale, the Fe–Mo oxide catalyst is easier to reduce to lower valance and the lattice oxygen ions in the oxide have a higher mobility. This may lead to the higher reactivity of lattice oxygen ions in the ultrafine oxide particles and, further, the higher selectivity to benzaldehyde.

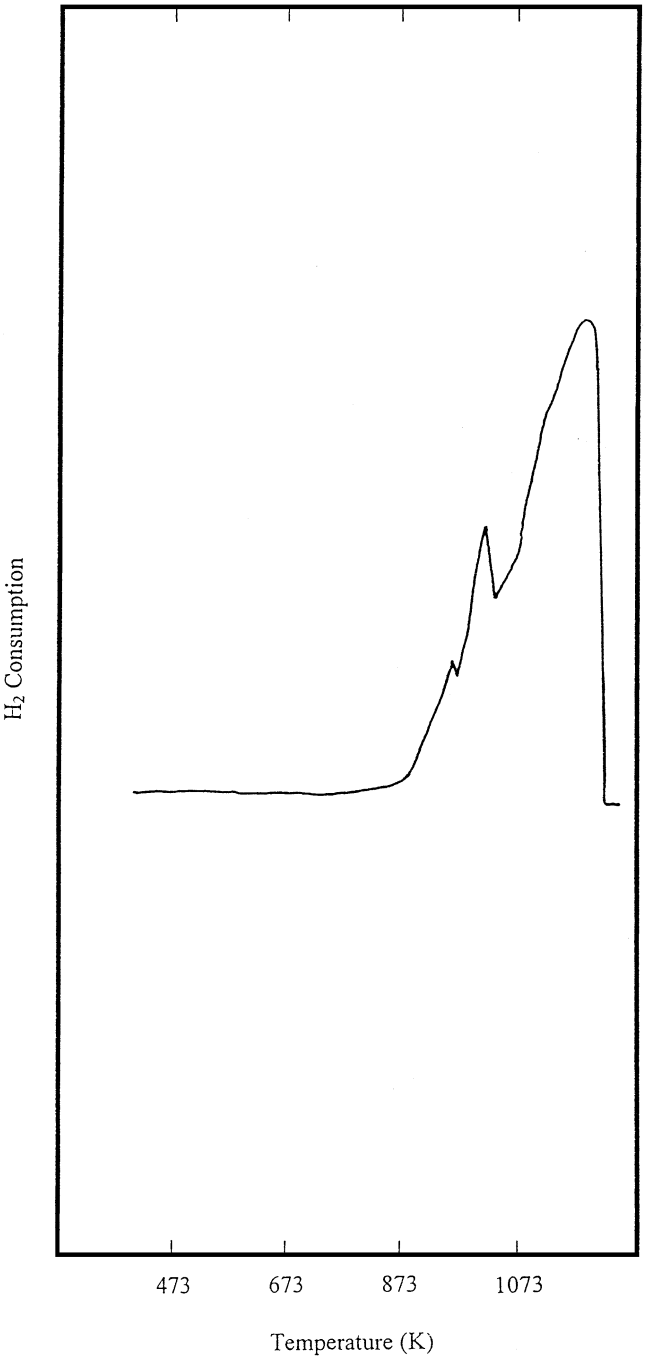

FIG. 3. TPR profiles of $Fe_2(MoO_4)_3$ catalysts prepared by the coprecipitation method (37).

The State and Reactivity of Lattice Oxygen Ions in the Ultrafine Mo-Based Oxides

The toluene oxidation reaction in the absence of molecular oxygen was used as a probe to evaluate the reactivity of lattice oxygen ions in the ultrafine Mo-based oxides. For partial oxidation of toluene to benzaldehyde in the absence of molecular oxygen, the reactivity of lattice oxygen ions in the ultrafine $Ce_2(MoO_4)_3$ is shown in Fig. 4. It can be seen that benzaldehyde is the main product and the selectivity is as high as ca. 95% every pulse. In contrast to the case in the presence of molecular oxygen (shown in Table 2), the selectivity to benzaldehyde is remarkably improved. This reveals that the lattice oxygen ions in the ultrafine $Ce_2(MoO_4)_3$ are the main active species for partial oxidation of toluene to benzaldehyde. In the absence of molecular oxygen, only lattice oxygen ions exist on the surface of the oxides, resulting in the higher selectivity to benzaldehyde.

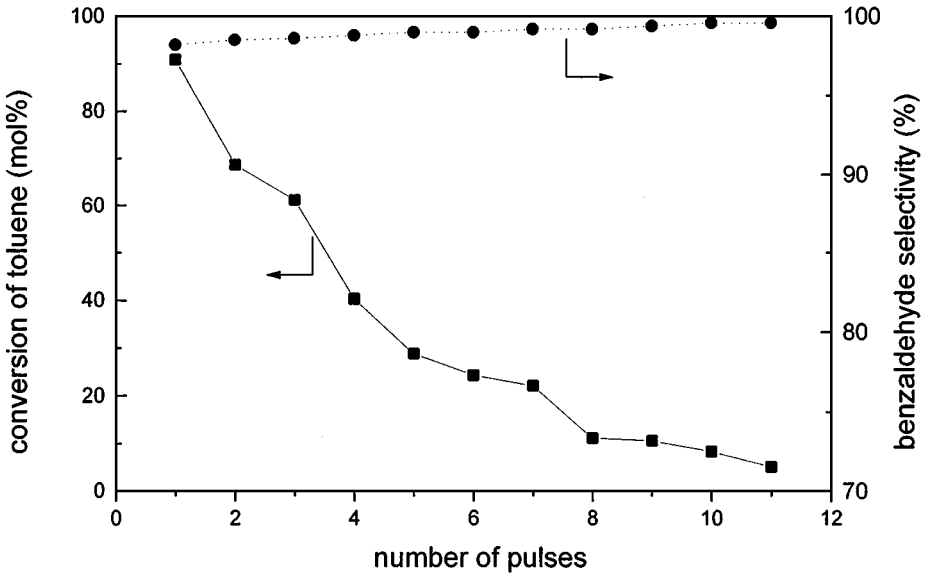

FIG. 4. The reactivity of lattice oxygen ions in the ultrafine $Ce_2(MoO_4)_3$.

The reactivity of lattice oxygen ions in the ultrafine Mo-based oxides is collected in Table 4. For mono-component Fe_2O_3, CeO_2, La_2O_3, and MoO_3 samples, no product is detected under our reaction conditions, indicating that in the absence of molecular oxygen the reactivity of lattice oxygen ions in these oxides is very low. As shown in Table 2, in the presence of molecular oxygen, Fe_2O_3, CeO_2, and La_2O_3 have highly catalytic activity for complete oxidation of toluene, which might be correlated to the strongly electrophilic oxidation ability of the oxygen species absorbed in the surface of these oxides.

Compared with that in mono-component oxides, the lattice oxygen ions in the ultrafine Mo-based oxides exhibit high reactivity for partial oxidation of toluene to benzaldehyde. This reveals that the addition of promoter oxides results in the high reactivity of lattice oxygen ions in the ultrafine mixed oxides. It is pertinent to note that the reactivity of lattice oxygen ions (the total amount of benzaldehyde yield) in the ultrafine Mo-based oxides follows the order $Ce_2(MoO_4)_3 > Fe_2(MoO_4)_3 > La_2(MoO_4)_3 \sim MoO_3$. This result is consistent with their selectivity to benzaldehyde in the presence of molecular oxygen, further suggesting that the lattice oxygen ions in the ultrafine Mo-based oxides are the main active species for partial oxidation of toluene.

TABLE 4

The Reactivity of Lattice Oxygen Ions in the Various Samples

Sample	Conversion of toluene (μmol g^{-1})[e]	Benzaldehyde selectivity (%)	Benzaldehyde yield (μmol g^{-1} m^{-2})[e]
Fe_2O_3[a]	0	0	0
CeO_2[a]	0	0	0
La_2O_3[b]	0	0	0
MoO_3[a]	0	0	0
$Fe_2(MoO_4)_3$[a]	1.1	92.0	0.05
$Ce_2(MoO_4)_3$[a]	12.1	98.5	0.59
$La_2(MoO_4)_3$[b]	—		—
$Fe_2(MoO_4)_3$[c]	0.01	91.2	0.004
$Ce_2(MoO_4)_3$[d]	0.19	88.9	0.04

Note. Dash indicates trace amount.
[a] Prepared by the sol–gel method and calcined at 673 K.
[b] Prepared by the sol–gel method and calcined at 773 K.
[c] Prepared by the coprecipitation method and calcined at 773 K.
[d] Prepared by the coprecipitation method and calcined at 823 K.
[e] The sum total of every pulse.

For comparison, the reactivity of lattice oxygen ions in the large $Fe_2(MoO_4)_3$ and $Ce_2(MoO_4)_3$ particles prepared by the coprecipitation method is also collected in Table 4. It is interesting to note that the reactivity of lattice oxygen ions in the large oxides is rather smaller than that in the ultrafine Mo-based oxides, which is consistent with their selectivity to benzaldehyde in the presence of molecular oxygen. This indicates that the lattice oxygen ions in the Mo-based oxides are the main active species for partial oxidation of toluene.

The state of lattice oxygen ions in the ultrafine $Ce_2(MoO_4)_3$ was further studied by employing a pulse microreactor combined with *in situ* Raman spectroscopy technique. In the absence of molecular oxygen, the influence of the pulse reaction of toluene upon the Raman spectra of $Ce_2(MoO_4)_3$ is presented in Fig. 5. The bands at 750–900 cm^{-1} may be assigned to Mo–O–Ce stretching vibrations, and the bands at 900–1000 cm^{-1} to Mo=O stretching vibrations (46–49). After reaction, while the actual band positions do not change among the samples, the relative intensities associated with the above bands do change. It can be found that in comparison with those of fresh sample,

after the twelfth pulse of toluene the bands assigned to Mo=O stretching vibrations almost disappear, while the intensities of bands attributed to Mo–O–Ce stretching vibrations almost do not change. If we combine this with the results of the reactivity of lattice oxygen ions in the ultrafine $Ce_2(MoO_4)_3$ (presented in Fig. 4), it may be concluded that the terminal Mo=O bonds are mainly responsible for the

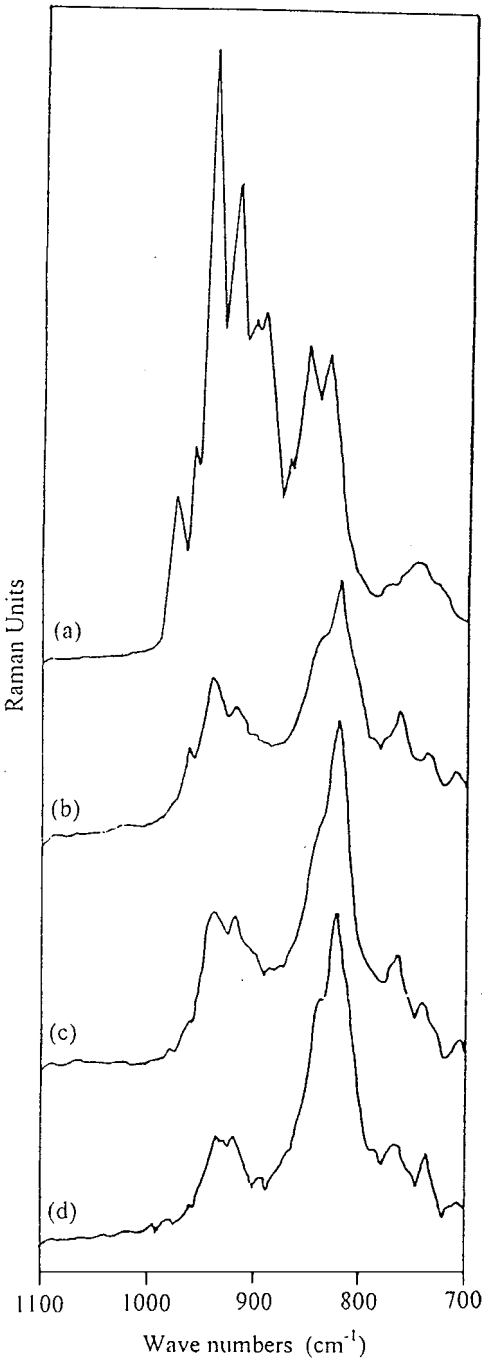

FIG. 5. *In situ* LRS spectra of ultrafine $Ce_2(MoO_4)_3$ for the reactivity of lattice oxygen ions: (a) fresh, (b) after the fourth pulse, (c) after the eighth pulse, (d) after the twelfth pulse.

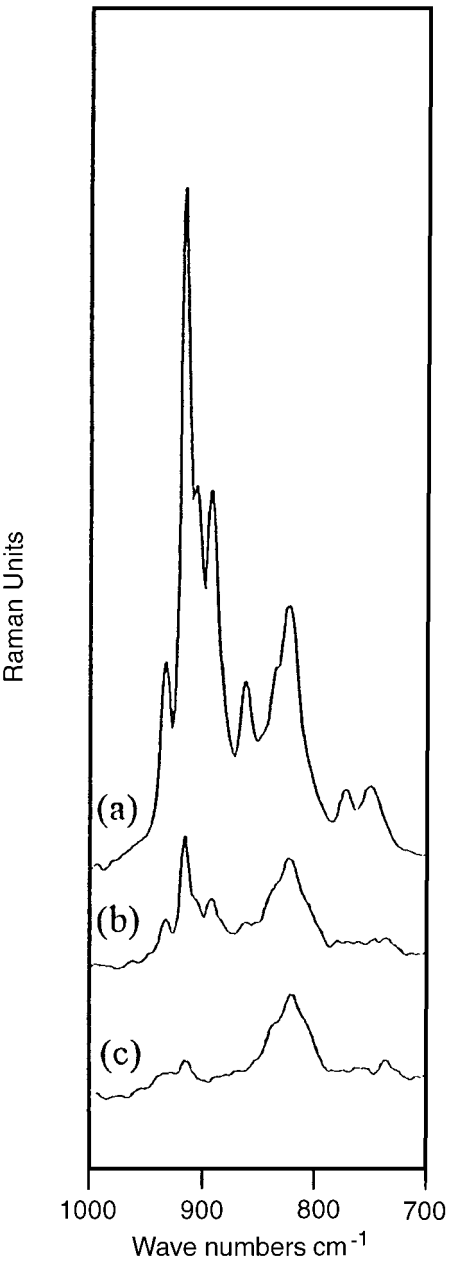

FIG. 6. *In situ* LRS spectra of $Ce_2(MoO_4)_3$ prepared by the coprecipitation method for the reactivity of lattice oxygen ions: (a) fresh, (b) after the fourth pulse, (c) after the eighth pulse.

reactive species for partial oxidation of toluene to benzaldehyde. Similar results can also be found from Fig. 6, which presents the influence of the pulse reaction of toluene upon the Raman spectra of $Ce_2(MoO_4)_3$ prepared by the coprecipitation method.

CONCLUSIONS

For partial oxidation of toluene to benzaldehyde, the ultrafine $Fe_2(MoO_4)_3$ and $Ce_2(MoO_4)_3$ particles exhibit

higher benzaldehyde selectivity and toluene conversion than the larger oxide particles prepared by the coprecipitation method. The unique catalytic properties of the ultrafine $Fe_2(MoO_4)_3$ and $Ce_2(MoO_4)_3$ particles may be correlated to the higher mobility of lattice oxygen ions in the oxides and their higher BET surface area. The addition of different promoter oxides results in different catalytic properties of the ultrafine Mo-based oxides. Cerium oxide is among the most effective promoter oxide for improving catalytic activity for partial oxidation of toluene to benzaldehyde. The selectivity to benzaldehyde follows the order $Ce_2(MoO_4)_3 > Fe_2(MoO_4)_3 > La_2(MoO_4)_3 > MoO_3$, which is in good agreement with the reducibility of Mo ions in the ultrafine Mo-based oxides. This result is also consistent with the reactivity of lattice oxygen ions in the ultrafine Mo-based oxides in the absence of molecular oxygen. These results indicate that the lattice oxygen ions in the ultrafine Mo-based oxides are the main active species for partial oxidation of toluene to benzaldehyde. Due to the formation of bicomponent oxides of $Fe_2(MoO_4)_3$, $Ce_2(MoO_4)_3$, and $La_2(MoO_4)_3$, the Mo ions in the ultrafine Mo-based oxides are easier to reduce to lower valance and the lattice oxygen ions in the oxides have a higher mobility. This leads to the higher reactivity of lattice oxygen ions in the ultrafine oxide particles and, further, the higher selectivity to benzaldehyde. The results of *in situ* LRS studies suggest that the terminal Mo═O bonds in $Ce_2(MoO_4)_3$ are the main reactive species for partial oxidation of toluene to benzaldehyde.

ACKNOWLEDGMENT

The support of the National Natural Science Foundation of China is gratefully acknowledged.

REFERENCES

1. van der Wiele, K., and van den Berg, P. J., *J. Catal.* **39**, 437 (1975).
2. Reddy, K. A., and Doraiswamy, L. K., *Chem. Eng. Sci.* **24**, 1415 (1969).
3. Germain, J. E., and Laugier, R., *C. R. Acad. Sci. Ser. C* **276**, 1349 (1973).
4. Ai, M., and Ikawa, T., *J. Catal.* **40**, 203 (1975).
5. Nag, N. K., Fransen, T., and Mars, P., *J. Catal.* **68**, 77 (1981).
6. Madhok, K. L., *React. Kinet. Catal. Lett.* **25**, 159 (1984).
7. Jonson, B., Rebenstorf, B., Larsson, R., Andersson, S. L. T., and Lundin, S. T., *J. Chem. Soc. Faraday Trans. I* **82**, 767 (1986).
8. Andersson, S. L. T., *J. Chem. Soc. Faraday Trans. I* **82**, 1537 (1986).
9. Grzybowska, B., Gzerwenka, M., and Sleezvnski, J., *Catal. Today* **1**, 157 (1987).
10. Jonson, B., Rebenstorf, B., Larsson, R., and Andersson, S. L. T., *J. Chem. Soc. Faraday Trans. I* **84**, 1897 (1988).
11. Jonson, B., Rebenstorf, B., Larsson, R., and Andersson, S. L. T., *J. Chem. Soc. Faraday Trans. I* **84**, 3363 (1988).
12. Jonson, B., Rebenstorf, B., Larsson, R., and Andersson, S. L. T., *J. Chem. Soc. Faraday Trans. I* **84**, 3547 (1988).
13. Yan, Z., and Andersson, S. L. T., *Appl. Catal.* **66**, 149 (1990).
14. Zhang, H., Zong, W., Duan, X., and Fu, X., *J. Catal.* **129**, 426 (1991).
15. Yan, Z., and Andersson, S. L. T., *J. Catal.* **131**, 350 (1991).
16. Das, A., Chatterji, S. K., and Ray, S. K., *Fuel Sci. Technol.* **10**, 85 (1991).
17. Barbaux, Y., Dejonghe, S., Gengenbre, L., and Grzybowska, B., *React. Kinet. Catal. Lett.* **47**, 1 (1992).
18. Matralis, H. K., Papadopoulou, C., Kordulis, C., Elguezabal, A. A., and Corberan, V. C., *Appl. Catal. A General* **126**, 365 (1995).
19. Elguezabal, A. A., and Corberan, V. C., *Catal. Today* **32**, 265 (1996).
20. Yoo, J. S., Lin, P. S., and Elfline, S. D., *Appl. Catal. A General* **124**, 139 (1995).
21. Yoo, J. S., *Appl. Catal. A General* **143**, 29 (1996).
22. Konietzni, F., Kolb, U., Dingerdissen, U., and Maier, W. F., *J. Catal.* **176**, 527 (1998).
23. Trifiro, F., *Catal. Today* **41**, 21 (1998).
24. Barnard, K. R., *J. Catal.* **125**, 265 (1990).
25. Itoh, H., Hosaka, H., Ono, T., and Kikuchi, E., *Appl. Catal.* **40**, 53 (1988).
26. Zhong, Z., Yan, Q., Fu, X., and Gong, J., *J. Chem. Soc. Chem Commun.*, 1745 (1996).
27. Liang, Q., Chen, K., Hou, W., and Yan, Q., *Appl. Catal.* **166**, 191 (1998).
28. Pajonk, G. M., *Appl. Catal.* **72**, 217 (1991).
29. Ward, D. A., and Ko, E. I., *Ind. Eng. Chem. Res.* **34**, 421 (1995).
30. Schneider, M., and Baiker, A., *Catal. Rev. Sci. Eng.* **37**, 515 (1995).
31. Zhong, Z., Chen, L., Yan, Q., and Fu, X., *Stud. Surf. Sci. Catal.* **91**, 647 (1995).
32. Stephens, H. P., Dosch, R. G., and Stohl, F. V., *Ind. Eng. Chem. Proc. Res. Dev.* **24**, 15 (1985).
33. Dutoit, D. C. M., Schneider, M., and Baiker, A., *J. Catal.* **153**, 165 (1995).
34. Kuang, W., Fan, Y., Yao, K., and Chen, Y., *J. Solid State Chem.* **140**, 354 (1998).
35. Kuang, W., Fan, Y., and Chen, Y., *Catal. Lett.* **50**, 31 (1998).
36. Kuang, W., Fan, Y., Chen, K., and Chen, Y., *J. Chem. Res.(s)*, 366 (1997).
37. Kuang, W., Fan, Y., and Chen, Y., *J. Colloid Interface Sci.* **215**, 364 (1999).
38. Zhang, H., Li, Z., and Fu, X., *Cuihua Xuebao* **9**, 331 (1988).
39. Shan, S., Chen, S., and Fu, Y., *Zhongguo Kexue Jishu Daxue Xuebao* **22**, 31 (1992).
40. Shen, J., Zhang, S., and Liang, D., *Cuihua Xuebao* **9**, 115 (1988).
41. Guerrero-Ruiz, A., Sepulveda-Escribano, A., and Rodriguez-Ramos, I., *Appl. Catal.* **120**, 71 (1994).
42. Smith, M. R., and Ozakan, U. S., *J. Catal.* **141**, 124 (1993).
43. Zhang, H., Shen, J., and Ge, X., *J. Solid State Chem.* **117**, 127 (1995).
44. Ge, X., Shen, J., and Zhang, H., *Sci. China Ser. B* **25**, 785 (1995).
45. Gopalakrishnan, J., and Manthiram, A., *J. Chem. Soc. Dalton Trans.*, 668 (1981).
46. Barraclough, C. C., Lewis, J., and Nyholm, R. S., *J. Chem. Soc.*, 3552 (1959).
47. Clark, G. M., and Doyle, W. P., *Spectrochim. Acta* **22**, 1441 (1966).
48. Trifiro, F., and Pasquon, I., *J. Catal.* **12**, 412 (1968).
49. Matsuura, I., *J. Catal.* **35**, 452 (1974).